



Tree Crown Size Estimated Using Image Processing: A Biodiversity Index for Sloping Subtropical Broad-Leaved Forests

Authors: Matsumoto, Hitoshi, Ohtani, Masato, and Washitani, Izumi

Source: Tropical Conservation Science, 10(1)

Published By: SAGE Publishing

URL: <https://doi.org/10.1177/1940082917721787>


BioOne Complete (complete.BioOne.org) is a full-text database of 200 subscribed and open-access titles in the biological, ecological, and environmental sciences published by nonprofit societies, associations, museums, institutions, and presses.

Your use of this PDF, the BioOne Complete website, and all posted and associated content indicates your acceptance of BioOne's Terms of Use, available at www.bioone.org/terms-of-use.

Usage of BioOne Complete content is strictly limited to personal, educational, and non - commercial use. Commercial inquiries or rights and permissions requests should be directed to the individual publisher as copyright holder.

BioOne sees sustainable scholarly publishing as an inherently collaborative enterprise connecting authors, nonprofit publishers, academic institutions, research libraries, and research funders in the common goal of maximizing access to critical research.

Tree Crown Size Estimated Using Image Processing: A Biodiversity Index for Sloping Subtropical Broad-Leaved Forests

Tropical Conservation Science
Volume 10: 1–12
© The Author(s) 2017
DOI: 10.1177/1940082917721787
journals.sagepub.com/home/trc


Hitoshi Matsumoto^{1,2}, Masato Ohtani^{3,4}, and Izumi Washitani^{1,5}

Abstract

Forest patches characterized by old trees with large crown sizes are of high biodiversity conservation value because they contain various microhabitats and may preserve the original flora of primeval or ancient forests. Aerial photo estimations of the average tree crown size represent a promising approach for identifying and monitoring such forest patches. Numerous sensors and algorithms have been developed to estimate the crown size in coniferous forests or forests with relatively low topographic variations; however, methods for estimating the crown size in steep broad-leaved forests in tropical or temperate regions are still required. We propose a method of estimating the size of tree crowns to obtain the “crown size index (CSI),” which can be used as a candidate biodiversity index for steep broad-leaved forest patches. We applied this method to a subtropical broad-leaved forest in southwestern Japan. In the first step, gray values from aerial imagery are converted to relative values, and then the crown size is subjected to a granulometric estimation. Regression of the CSI from the diameter at breast height of the canopy layer trees presented R^2 values as high as 0.67. Resampling tests revealed that monochrome aerial images resampled with spatial resolutions ranging from 0.40 m to 1.20 m produced results with relatively high accuracy ($R^2 \geq .55$). These results suggest that the proposed method has the potential for use as a cost-effective method of evaluating the biodiversity of broad-leaved forest patches in hilly or mountainous regions using images from various high-resolution sensors.

Keywords

cost-efficient evaluation of forest biodiversity, protected area, granulometry, high-resolution imagery, forest on steep hills or mountains

Forest crown size is a key structure related to ecosystem functions, such as timber production, nutrient cycling, and carbon storage (Song, Dickinson, Su, Zhang, & Yaussey, 2010), which are of considerable concern to human societies. Crown size is also related to forest mosaic patch biodiversity (Bengtsson, Nilsson, Franc, & Menozzi, 2000; Nagendra et al., 2013), which shifts dynamically according to both human interventions and natural disturbances (Pickett & White, 1985).

Because of the allometric relationships among tree structure variables (Kira & Shidei, 1967), a forest patch characterized by a large crown size is likely to have a high proportion of old trees and include old-growth or mature forest patches that have escaped major human interventions for a relatively long time (Burrascano, Keeton, Sabatini, & Blasi, 2013; Whitman & Hagan, 2007). Such forest patches may have a high biodiversity value because highly developed complex structures of both living and dead trees generate a large variety of microhabitats for plants and animals, including tree hollows

and coarse woody debris rotting to various degrees (Brokaw & Lent, 1999; Cockle, Martin, & Robledo, 2012; Kruys, Fries, Jonsson, Lämås, & Ståhl, 1999; Nilsson et al., 2002; Speight, 1989; Stokland, Siitonen, & Jonsson, 2012; Winter & Möller, 2008). These

¹Graduate School of Agricultural and Life Sciences, The University of Tokyo, Japan

²GPS Co. LTD., Saitama, Japan

³Hokkaido Regional Breeding Office, Forest Tree Breeding Center, Forestry and Forest Products Research Institute, Hokkaido, Japan Present address

⁴Section of Nature and Environment, Institute of Natural and Environmental Sciences, University of Hyogo, Japan

⁵Laboratory of Conservation Ecology, Department of Integrated Science and Engineering for Sustainable Society, Faculty of Science and Engineering, Chuo University, Tokyo, Japan

Received 21 March 2017; Revised 21 May 2017; Accepted 26 June 2017

Corresponding Author:

Hitoshi Matsumoto, GPS Co. Ltd, 942-1 Sueda, Iwatsuki-ku, Saitama, Saitama 339-0021, Japan.

Email: matsumoto.hitoshi132@gmail.com



Creative Commons CC-BY: This article is distributed under the terms of the Creative Commons Attribution 4.0 License (<http://www.creativecommons.org/licenses/by/4.0/>) which permits any use, reproduction and distribution of the work without further permission provided the original work is attributed as specified on the SAGE and Open Access pages (<https://us.sagepub.com/en-us/nam/open-access-at-sage>).

microhabitats can provide vertebrates, invertebrates, plants, bryophytes, lichens, and fungi with food, nests, and regeneration substrates (Butin & Kowalski, 1983; Jonsell, Hansson, & Wedmo, 2007; Kennedy & Quinn, 2001; Speight, 1989; Stokland et al., 2012; Takahashi, Sakai, Ootomo, & Shiozaki, 2000).

Moreover, old-growth patches that have escaped major disturbances may preserve flora of high conservation value (Honnay, Degroote, & Hermy, 1998) known as “ancient forest species,” which are characterized by a high shade tolerance, low colonizing ability, and preference for mesic environments (Bossuyt, Heyn, & Hermy, 2002; Brown & Oosterhuist, 1981; Hermy, Honnay, Firbank, Grashof-Bokdam, & Lawesson, 1999; Peterken, 1974; Whitney & Foster, 1988).

In recent years, a number of researchers have attempted to estimate tree crown size with various algorithms and high spatial resolution aerial or satellite images (Culvenor, 2002; Hirata, 2008; Leckie, Gougeon, Walsworth, & Paradine, 2003; Song & Woodcock, 2003; Wang, Gong, & Biging, 2004; Wulder, Niemann, & Goodenough, 2000). Irrespective of the target and the purpose of the estimation, these efforts have generally employed two-step algorithms, with tree crown detection as the first step and crown delineation as the second step (Ke & Quackenbush, 2011). Tree crown detection algorithms detect treetops based on the local maximum of gray values, whereas delineation algorithms define the outline of tree crowns by delineating the valleys of gray values because gray values are higher at treetops, which reflect more solar light and are lower toward crown boundaries.

Most previous studies have focused on coniferous plantations or relatively homogenous high-latitude boreal forests consisting of conical crown trees on flat land, that is, a forest with relatively low topographic variations (Ke & Quackenbush, 2011), and few studies have attempted to estimate the tree crowns of primeval or secondary tropical to temperate forests of high biodiversity value, which primarily consist of broad-leaved trees with a greater variety of species and ages.

Compared with conical crowns where the tops and boundaries are easily detectable in remotely sensed imagery, the tops or boundaries of irregularly shaped crowns of broad-leaved trees are difficult to identify. As such, the algorithms developed for conifer forests are less effective for broad-leaved trees. Song (2007) and Song et al. (2010) estimated the average tree crown size on a forest stand basis based on the behavior of image semivariograms at different spatial resolutions of satellite imagery of North American forests and reported a considerably higher accuracy for average tree crown size estimations of a conifer stand ($R^2 = .73$) than of a broad-leaved stand ($R^2 = .60$).

Moreover, heterogeneity in the species, age, and arrangement of the trees in natural forests increase the difficulty of performing estimations (Ke & Quackenbush,

2011; Pouliot & King, 2005). To overcome the problems caused by highly heterogeneous crown structures, the use of granulometry, a pixel-basis algorithm, is a promising alternative. Heinzl, Weinacker, and Koch (2011) employed this method to estimate the crown size of a flat deciduous forest in Europe. Matsumoto, Ishii, Ohtani, and Washitani (2014) also delineated single crowns using an object-based image analysis and estimated the average crown size in a flat beech forest in northern Japan, and the regression accuracy for the estimated average tree crown size based on the average of canopy tree diameter at breast height (DBH) measured in the field was $R^2 = .55$. These pixel-based methods can be applied to forest patches with unclear stand boundaries.

Previous studies have developed algorithms that are primarily applicable to flat forests with simple topographies. However, forests that are important from a biodiversity perspective in subtropical or temperate regions, such as Japan, Europe, and eastern North America, are primarily located in remote hills or mountains free from most human interventions (Biodiversity Center of Japan, 2010; Peterken, 1996). In the tropics, most lowland natural forests have been lost (Turner & Corlett, 1996), and there is growing concern for the conservation of mountainous forests. To meet the growing needs for biodiversity evaluations of such natural and secondary forests, cost-efficient algorithms for estimating crown size that can be applied to broad-leaved forests in hilly or mountainous regions with complicated topographies must be developed.

In this study, we attempted to develop a two-step method of estimating the average tree crown size in mature or secondary broad-leaved forest patches on steep hills using high spatial resolution aerial photographs. We first developed an image conversion algorithm to treat varying patterns of brightness or shadows in remotely sensed images of steep forests with slopes that differ greatly in direction. These converted images were processed by granulometry to estimate the tree crown size (pixel-based crown size index [CSI]).

To use crown size as an index for biodiversity evaluations, determining the size for each single crown is not always necessary, and the average or representative value for forest patches may be more appropriate. The representative tree crown size within a certain region can be acquired by averaging the pixel-based CSI in the region. We tested the validity of this method against the tree size parameter measured on the ground.

The chosen study site is an evergreen broad-leaved forest in the steep hills of Amami Oshima Island, southwestern Japan. The “subtropical forests of Nansei Islands,” including Amami Oshima Island, are one of the world’s biodiversity hotspots (Rodrigues et al., 2004), and a plan to establish a new forest nature reserve system in central Amami Oshima Island has been

considered by the Ministry of the Environment (Naha Nature Conservation Office, 2008) to designate Amami Gunto National Park in 2017. The method proposed here could be used not only at the planning stage to select the appropriate protected areas for a nature reserve but also after the establishment to periodically monitor the area.

Method

Study Area

The study site is located in Kinsakubaru National Forest (28.320°N ~ 28.356°N, 129.439°E ~ 129.464°E, 477 ha) on the central Amami Oshima Island (Figure 1). The zone at 165 m ~ 450 m above sea level is covered with a mosaic of mature and secondary patches of East Asian subtropical-type evergreen broad-leaved forest (Ohsawa, 1990; Tagawa, 1995). The canopies of mature and secondary forest patches are dominated by *Castanopsis sieboldii* (Makino) Hatus. ex T. Yamaz. et Mashiba and *Schima wallichii* (DC.) Korth. subsp. *noronhae* (Reinw. ex Blume) Bloemb., which grow on steep slopes with highly variable azimuths (Figure 2). The crown diameters of canopy layer trees in this study area ranged from approximately 1 m to 8 m, and the tree density of canopy layer trees ranged from approximately 350 to 4000 per ha. The canopies of the patches are largely closed regardless of the length of time since the last clear-cut.

Aerial Photograph

A digital color (Blue-Green-Red [BGR]) aerial photograph was taken by the Geospatial Information Authority of Japan at 10:32 + 0900 (Japan Standard Time [JST]), December 3, 2008, with a solar azimuth

angle of 152°. This image was taken at a scale of 1:20,000, and the ground sample size for each pixel was 0.40 m.

We excluded areas without tree crowns, such as roads or grasslands, and the area where single tree crowns could not be recognized because of deep shadows caused by topography. The accuracies of CSIs estimated from spectral bands were compared, and we only used Band 2 (green), which is generally selected for processing natural color imagery (Ke & Quackenbush, 2011) for further

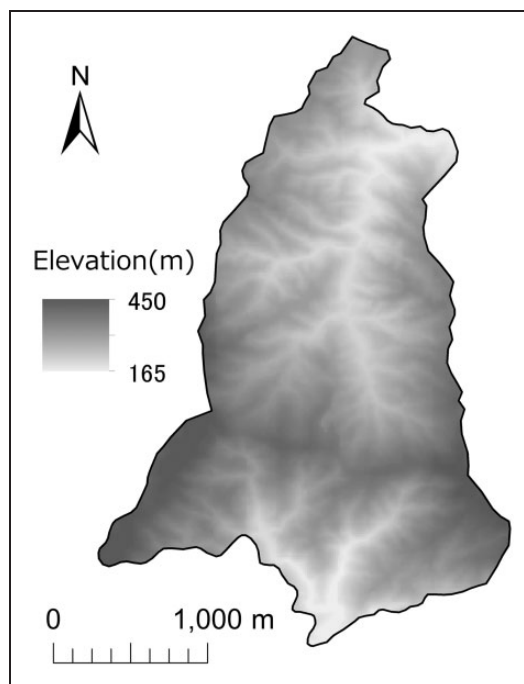


Figure 2. Elevation of Kinsakubaru National Forest.

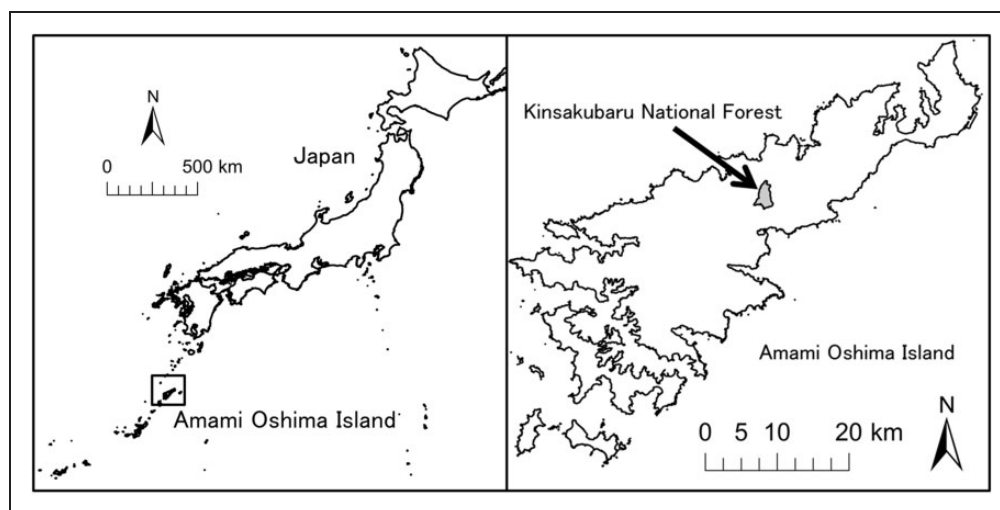


Figure 1. Location of Amami Oshima Island and Kinsakubaru National Forest.

analyses. The image was georeferenced manually with six ground control points (the root-mean-square error was 1.4 m).

Image Processing

We adopted an image processing algorithm to simplify the highly variable patterns of brightness or shadows in the remotely sensed imagery of variably sloping forests. After this conversion, we estimated the tree crown size using granulometry and tested the validity of the procedure through a regression on field-measured tree size data.

Image conversion for reducing slope azimuth effects. In an aerial image of forest patches on steep hills, the solar incident angle into the canopy surface varies depending on the slope azimuthal angle, which leads to varying patterns of brightness or shadows. With such aerial images, it is difficult to apply a uniform algorithm to the entire image. However, within the scope of a few crowns (25 pixels/circle in this case, which is referred to as the neighboring domain, D , below), the basic pattern of brightness or darkness is common regardless of the slope azimuth; therefore, the gray values are higher near treetops and lower around crown boundaries. In the following Equation 1, we converted the original gray values to relative values that represent the relative brightness within the scope of a few crowns around each pixel.

$$X = k \left(\mu + F^{-1} \left(\frac{k-1}{20} \right) \sigma \leq x < \mu + F^{-1} \left(\frac{k}{20} \right) \sigma \right), \quad (1)$$

($k = 1 \sim 20$)

where X is the relative gray value, x is the original gray value, k is an integer value, F is the cumulative distribution function of standard normal distribution, μ is an averaged original gray value within the neighboring domain D , and σ is the standard deviation of original gray value within D .

The mean μ and the standard deviation σ of the original gray value x were calculated for each pixel within the neighboring domain D . D is circular with a radius of 25 pixels (10 m). This method supposes that both treetops and crown boundaries are included in a single neighboring domain, that is, D must not be included within a single tree crown. Our visual observation of the aerial photograph ascertained that a radius of 25 pixels is large enough to include at least the two largest tree crowns. The probability variables that divide the cumulative distribution of the Gaussian distribution with the mean μ and the standard deviation σ into 20 parts were calculated. The smallest of these probability variables that was greater than x was designated as the relative gray value ($1 \leq X \leq 20$). The original and the converted image of the representative aerial photograph scene are shown in Figure 3.

Granulometry. The tree crown size was estimated using the granulometry method, which calculates a size distribution of grains in the images based on the mathematical morphology (Heinzel et al., 2011). In our study, individual tree crowns and crown boundaries were regarded as the grains and the background, respectively. The two basic mathematical morphology operations are erosion and dilation. These operations process gray values within a structural element (SE), which is represented by an image with a certain shape and

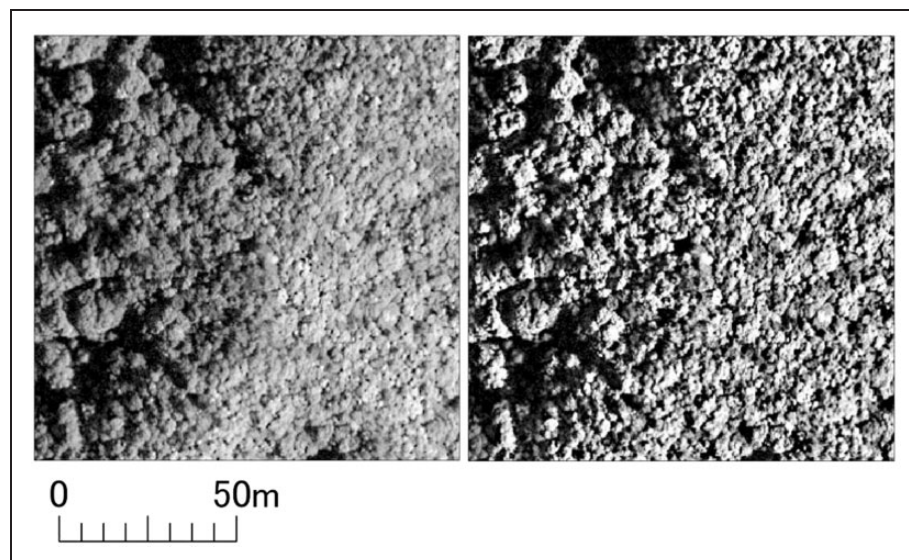


Figure 3. Aerial images with (right) or without (left) image conversion by the processing algorithm described in the text.

size. Erosion assigns the minimum gray values within the SE to the center pixel, and dilation assigns the maximum values to the center pixel (Soille, 2004). The process of erosion followed by dilation is called opening, and it eliminates objects smaller than the SE in the image (Figure 4).

Granulometry deduces the dominant object size within a moving window by comparing the sum of the gray values of the opened and original imagery. In our study, we applied a circular moving window with a 15-pixel (6.0 m) radius as S . The 15-pixel radius was large enough to include the largest tree crown in our study site.

Both converted and nonconverted aerial photographs were opened with 10-size classes of circular SEs whose radius λ ranged from 1 pixel (0.40 m at the ground level) to 10 pixels (4.0 m). The center of the SE was positioned at every pixel of the image. The size range of the SEs conformed well to the crown size in the study site. A preliminary analysis showed that when the SE had a radius greater than 10 pixels, it caused more outliers because it included apparently merged crowns or relatively bright matrices, such as canopy gaps. In a forest where the crown size of the canopy layer trees is heterogeneous, a larger moving window not only demands greater computational effort but also includes different forest patches, which results in larger estimation errors.

The ratio $R_S(\lambda)$ is the sum of the gray values of the opened image with an SE of radius λ divided by the sum of the gray values of the original image in the moving window S . Figure 5 shows the $R_S(\lambda)$ plotted against λ for the image of Figure 4. The $R_S(\lambda)$ decreases as the SE expands, and the decrease reaches a peak value when the size of the SE best fits the dominant object size within the moving window. The crown size at a particular pixel, which is referred to below as the pixel-based CSI, was estimated as the moving window size λ that caused the maximum decrease of the $R_S(\lambda)$.

Image resampling. To evaluate the range of pixel sizes over which the proposed method is useful, we resampled the Band 2 imagery, and the accuracy of the estimations was

compared. The original imagery was resampled to generate a series of six images that had pixel sizes of 0.60×0.60 , 0.80×0.80 , 1.20×1.20 , and 1.60×1.60 m. The gray value of the resampled pixel was the average of the gray values of the original pixels (Jones & Vaughan, 2010), except for the pixel size of 0.60, which is not an integral multiple of the original pixel size. For the pixel size of 0.60 m, we used the bilinear interpolation method, which calculates the distance-weighted average of the four nearest pixels. Each resampled image was converted to relative gray values, and the CSI was calculated.

We used the Spatial Analyst extension of ArcGIS 10 (Esri Inc., Redlands, CA) for the aerial imagery processing.

Field Measurement

To collect ground reference data on the size of the canopy layer trees, we conducted field measurements from

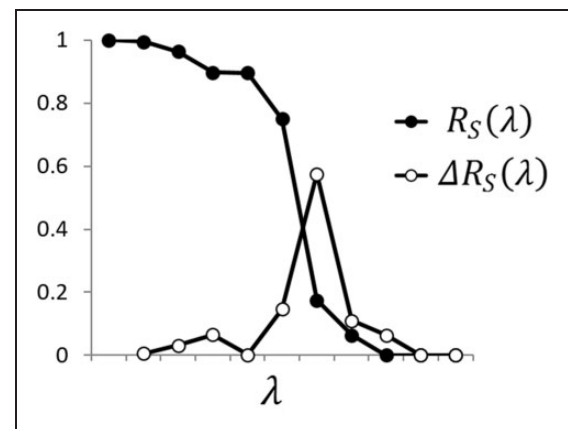


Figure 5. An example of granulometric analysis on the image from Figure 4. Plot of the sum of the gray values of the opened image divided by the sum of the gray values of the original image ($R_S(\lambda)$) and the difference ($\Delta R_S(\lambda)$) with regard to the radius of the structuring element (λ).

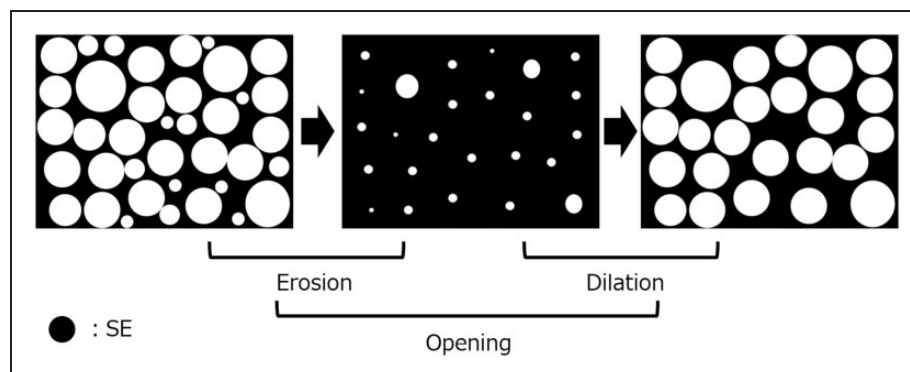


Figure 4. Operations of mathematical morphology for a specific structuring element. Binary images are shown for demonstration.

November 25 to December 6, 2013, from February 24 to March 2, 2014, and from November 18 to November 22, 2014. A total of 22 sampling plots were outlined based on our visual observation of the aerial photograph prior to the field measurement and were recorded in the GPS (GeoExplorer 6000 series handheld, Trimble, CO). The study area had not experienced any large human or natural disturbances, such as forest fire or landslide, since 2008, when the aerial photograph was taken. Each plot was located in mature forest patches or secondary forest patches with a closed canopy, where the average size of the canopy layer trees was relatively uniform. Sampling plots were square or rectangular with an area of 1 ha.

Because of the steep slopes and the existence of dangerous venomous snake *Protobothrops flavoviridis*, it was difficult to collect ground reference data over large continuous areas or to measure the crown size of every tree; therefore, we set up two 100 m² quadrats in each plot and measured the DBH of all canopy layer trees in the quadrats. Each plot was located on microtopographies, where we can conduct field measurements safely (mostly on slopes with an angle of 10–44°) and where the tree size was representative of the forest stand. To avoid the influence of canopy change due to finer natural disturbances, such as strong winds since 2008, we did not set quadrats in canopy gaps that are not recognized in the aerial photograph. The location of each quadrat was recorded with GPS.

Statistical Analyses

The CSI estimated at each pixel size was averaged within each sampling plot (converted_{0.40}, converted_{0.60}...converted_{1.60}). The estimated CSI of the nonconverted imagery was also averaged within each sampling plot (original_{0.40}).

To evaluate the effectiveness of the image conversion, we performed a series of regression analyses between the logarithm of the averaged DBH and the logarithm of the CSI. The allometric relationships between DBH and crown diameter are species and site specific (Dietze, Wolosin, & Clark, 2008; Song et al., 2010). However, in our study site, it is not realistic to construct allometric models for all canopy layer species because of the high diversity of canopy layer species and difficulties of data collection due to steep topographies. Allometric relationships are known to differ among life history traits in some tropical or warm-temperature broad-leaved forests (Aiba & Kohyama, 1997; Iida et al., 2011). The dominant species, *C. sieboldii* and *S. wallichii* subsp. *noronhae*, are both evergreen broad-leaved trees that construct subtropical mature forest, while pioneer species with wider crowns, such as charcoal-tree (*Trema orientalis* L.) or Luchu pine (*Pinus luchuensis* Mayr.), are rare in the canopy layer, and

so approximation by log-log relationship was applied between the plot mean CSI and the plot mean DBH.

We first compared the R^2 of the regression analyses with or without image conversion. The influence of slope direction on the estimation results was subsequently examined. A multiple regression analysis was conducted with the logarithm of converted_{0.40} as the response variable and the logarithm of the averaged DBH and the cosine of the angle formed by the solar azimuth and slope direction (COS) as the explanatory variables. The COS takes a higher value when the slope direction is consistent with the solar azimuth angle, and it was calculated within the sampling plot using a 10-m digital elevation model (DEM).

The R^2 of the regression between the logarithm of the averaged DBH and the logarithm of the averaged CSI estimated with aerial images of different pixel sizes was also compared.

Statistical analyses were conducted with ArcGIS 10 (ESRI Inc., Redlands, CA) and R 3.0.1 (R Development Core Team, 2013).

Results

Effectiveness of Image Conversion

We sampled a total of 562 canopy layer trees (49 species). There were 547 trees (44 species) that were evergreen broad-leaved trees, 9 trees were deciduous broad-leaved trees (4 species: *Cordia dichotoma* G.Forst., *Idesia polycarpa* Maxim., *Styrax japonica* Siebold et Zucc., and *Toxicodendron succedaneum* (L.) Kuntze), and 6 trees were evergreen coniferous trees (1 species: *Nageia nagi* [Thunb.] Kuntze). There were 241 trees (42.9 %) that were *C. sieboldii*, and 82 trees (14.6 %) were *S. wallichii* subsp. *noronhae*, while the proportion of every other species was less than 5%. The averaged DBH of all the recorded trees was 20 cm. The maximum value, 75th percentile, median, 25th percentile, and minimum value of the DBH were 93 cm, 25 cm, 16 cm, 10 cm, and 2 cm, respectively. The average, maximum value, median, and minimum value of the number of trees within the two quadrats in each plot was 26, 80, 18, and 7, respectively. The maximum value, median, and minimum value of the averaged DBH in each plot were 50 cm, 25 cm, and 10 cm, respectively.

Double logarithmic plots of the DBH of the canopy layer trees and the averaged CSI are shown in Figure 6. The regression analysis showed that the converted_{0.40} values calculated using each spectral band had significant positive correlations with the averaged DBH of the canopy layer trees. The R^2 of the regression was the highest for Band 2 (0.67) and the lowest for Band 3 (0.56). The original_{0.40} had significant positive correlations with the averaged DBH for only Band 1, and the R^2 was lower for every spectral band than for the converted_{0.40} (Table 1).

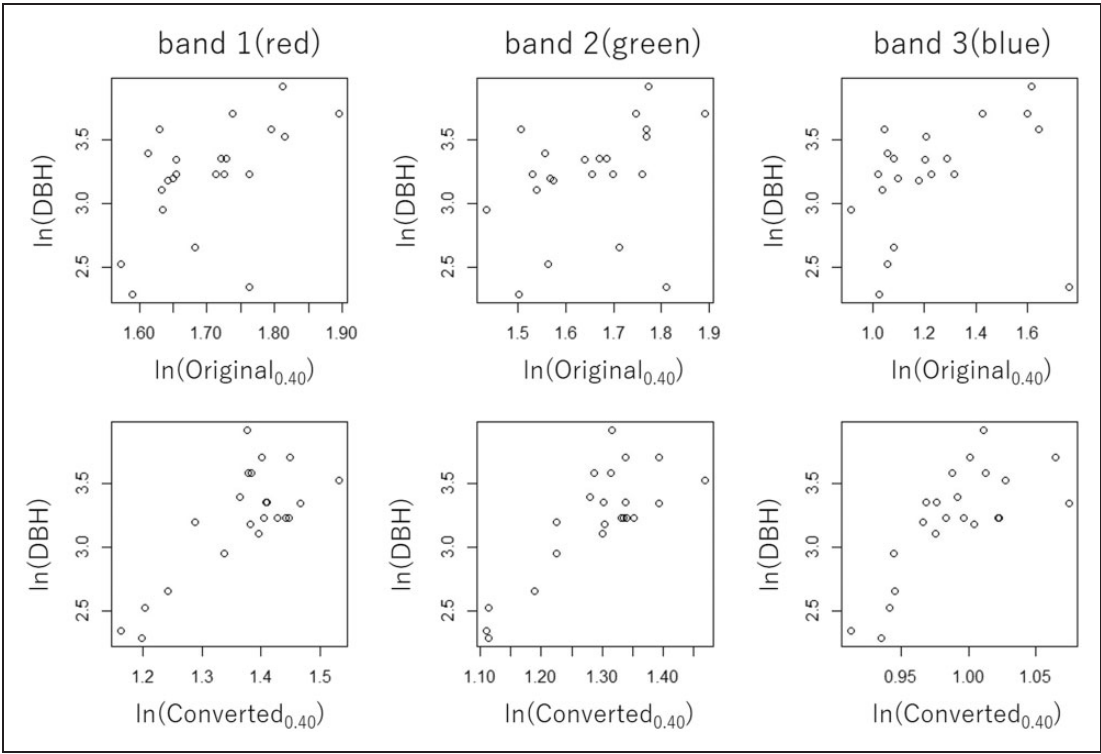


Figure 6. Plot of the logarithm of the averaged diameter at breast height against the logarithm of the converted_{0.40} (lower) and original_{0.40} (upper) values.

Table 1. Results of the Double-Logarithmic Regressions of the DBH of the Canopy Layer Trees on the Averaged CSI for Each Spectral Band.

coefficients	Explanatory variable					
	log(Converted _{0.40})			log(Original _{0.40})		
	Band 1	Band 2	Band 3	Band 1	Band 2	Band 3
<i>B</i>	3.624	3.788	7.896	2.752	1.208	.503
<i>SE</i>	0.628	0.594	1.581	0.986	0.757	.383
<i>p</i>	<.001	<.001	<.001	.01	.13	.2
<i>R</i> ²	.62	.67	.56	.28	.11	.08

Note. Converted_{0.40} was calculated using the converted imagery and Original_{0.40} was calculated using the nonconverted imagery. DBH = diameter at breast height; CSI = crown size index; B = regression coefficient; SE = standard error.

The multiple regression analysis showed that the DBH was the only parameter with a significant positive correlation with the averaged CSI for Band 2 ($\beta = .173$, $p < .001$). The COS was not significantly correlated with the averaged CSI ($\beta = -.011$, $p = .62$). As shown in Figure 7, the COS showed a significant positive correlation with the difference between the original_{0.40} and converted_{0.40} values of Band 2 ($\beta = .798$, $p < .001$).

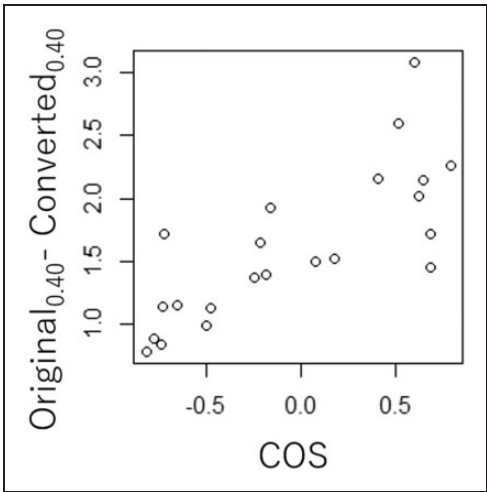


Figure 7. Plot of the difference between the original_{0.40} and converted_{0.40} values against the cosine of the angle formed by the solar azimuth and slope direction.

Original_{0.40} tended to be overestimated where the slope faced the sun.

Estimation at Different Pixel Sizes

The resampled images are shown in Figure 8. The 0.40-m-pixel size image is able to differentiate a forest patch on

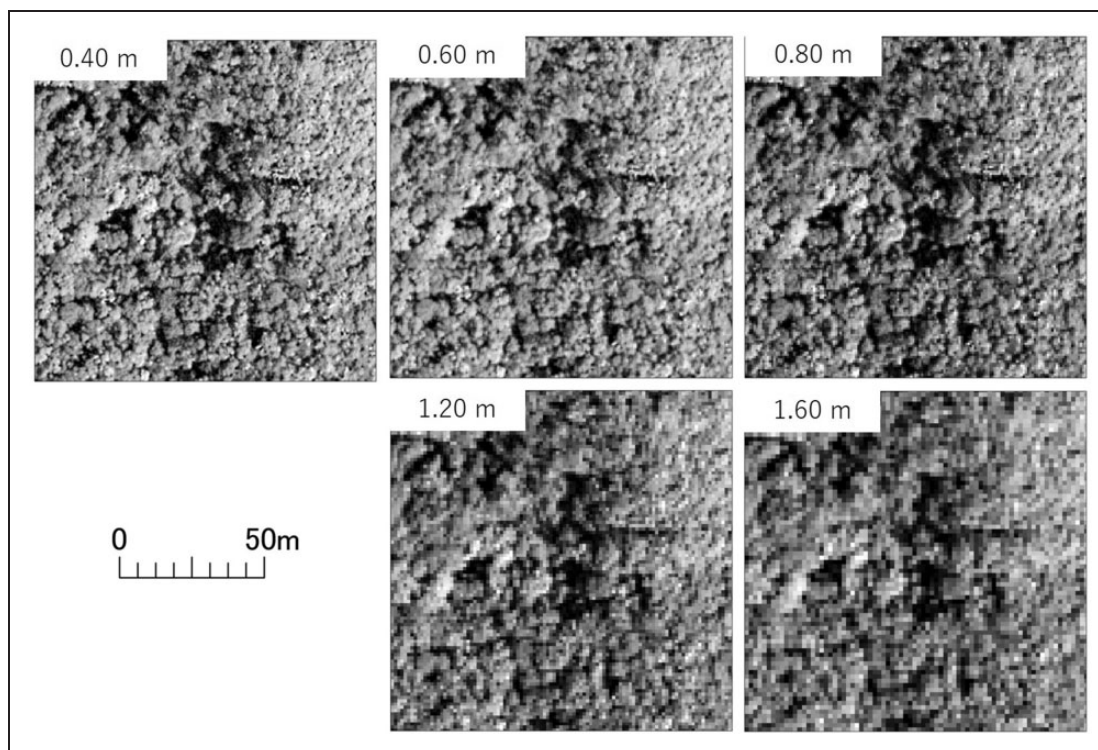


Figure 8. Aerial images resampled with different pixel sizes. Pixel sizes are shown at the upper left of the images.

the right side that was composed of smaller trees; however, smaller trees are not discernible as single objects, and the crown boundaries of larger trees become obscure in coarser images. For example, a tree crown with a diameter of 1.5 m is composed of 11 pixels in the 0.40-m pixel size image, whereas it is composed of less than a single pixel in the 1.60-m pixel size image. The series of double-logarithmic regression analyses showed that each averaged CSI for Band 2 had a significant relationship with the DBH of the canopy layer trees. The R^2 of the regression declined as the image became coarser and dropped below 0.50 at the 1.60-m pixel size (Figure 9, Table 2).

Discussion

Effectiveness of Image Conversion

The image conversion algorithm adopted here satisfactorily improved the estimation accuracy of the average tree crown size in a forest patch on steep hills, and the slope direction did not have a significant effect on the results. With nonconverted imagery, a marked overestimation of the tree crown size on slopes facing the sun was apparent, which may reflect differing patterns of shadows created by solar light entering at different incident angles. On a slope facing the sun, the solar light enters the canopy surface with an incident angle close to perpendicular; therefore, the area reflecting solar light is larger (even

on crown boundaries), and the crown area may be overestimated or several crowns may be merged together because the shadows on the crown boundaries are obscured. However, on a slope opposite from the sun, the solar light enters the canopy surface sideways; therefore, less solar light enters the crown boundaries, and the crown size could be underestimated because of larger shadows between the tree crowns. The image conversion performed in this study satisfactorily enhanced the estimation accuracy by highlighting shadows between crowns on slopes facing the sun and by increasing the brightness of crown boundaries on shady slopes.

Few studies have tried to estimate the average tree crown size in broad-leaved forests (Ke & Quackenbush, 2011), and the estimation accuracy was lower compared to coniferous forests. Matsumoto et al. (2014) reported an R^2 of .55 in a double logarithmic regression analysis between the field-measured DBH and the estimated tree crown area using object-based image analysis. Song et al. (2010) reported an R^2 of .60 in a broad-leaved stand and an R^2 of .73 in a coniferous stand. Although our R^2 cannot be simply compared to the R^2 of Song et al. (2010), where allometric parameters between the DBH and the crown diameter were calculated for each tree species, our method can be a practical means of vegetation mapping to find forest stands characterized by large crown diameters in a steep broad-leaved forest. Future studies are needed to ascertain the effectiveness of this

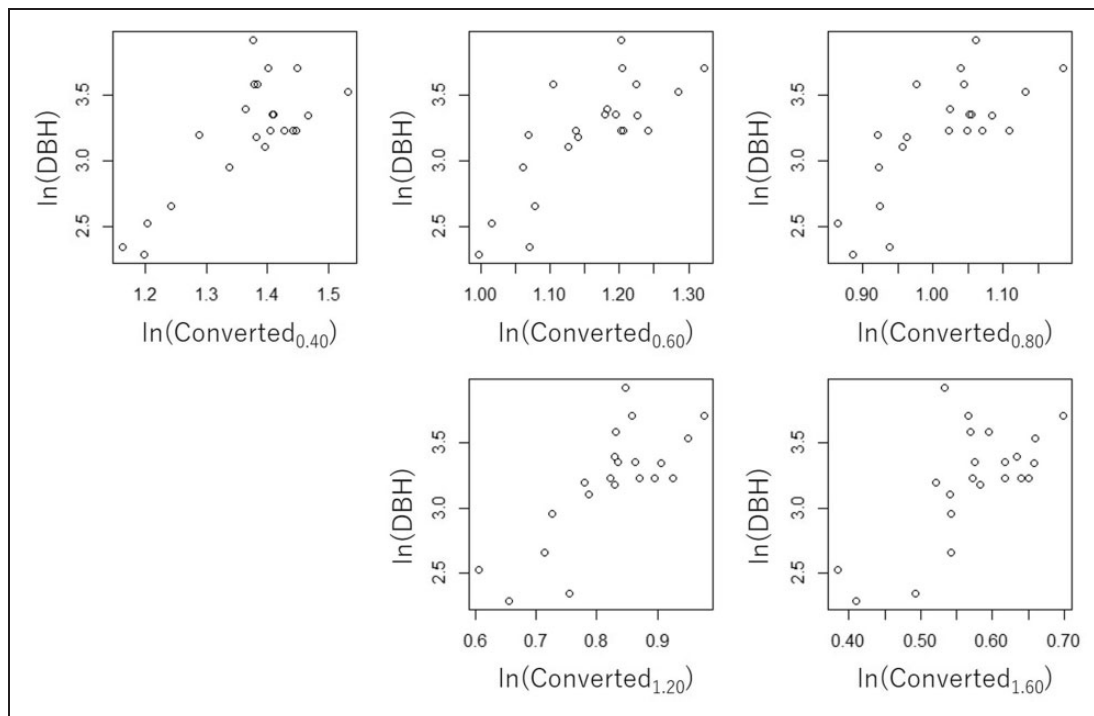


Figure 9. Plot of the logarithm of the averaged diameter at breast height against the logarithm of averaged crown size index at different pixel sizes.

Table 2. Results of the Double-Logarithmic Regressions of the DBH of Canopy Layer Trees on the Averaged CSI Calculated With the Band 2 Images of Different Pixel Sizes.

Pixel size (m)	0.4	0.6	0.8	1.2	1.6
<i>B</i>	3.788	3.955	3.834	3.661	3.793
<i>SE</i>	0.594	0.71	0.775	0.679	0.917
<i>p</i>	<.001	<.001	<.001	<.001	<.001
<i>R</i> ²	.67	.61	.55	.59	.46

Note. DBH = diameter at breast height; CSI = crown size index; SE = standard error.

method as a biodiversity index through application over a regional scale and comparing to the spatial biodiversity patterns that have been recognized by other data sources.

Estimation at Different Spectral Bands or Different Pixel Sizes

The R^2 of the regression analysis was the highest for Band 2 (green), suggesting that the relatively high reflectance of green light from forest canopies highlighted the gray-value differences between treetops and crown boundaries.

The R^2 of the regression declined with increasing pixel size, especially for the image with a pixel size of 1.60 m. Generally, in an image of larger pixel sizes, crown boundaries are obscure, and smaller crowns cannot be

recognized as a single object. In our study area, the smallest crowns are difficult to be discerned in the 0.80-m pixel size images, but the plots with smaller DBH showed lower CSI in the images with a pixel size smaller than 0.80 m, while some plots with a smaller DBH in the images of a 1.20-m or 1.60-m-pixel size showed relatively high CSI (Figure 9). In a 0.80-m pixel size image, even if individual crowns cannot be discerned, then the gray value of each pixel retained part of the reflection patterns formed by the treetops and crown boundaries (Figure 8). The tree crowns are apparently merged together in an image whose pixel size is larger than the tree crown size because the gray value of a pixel is made up of the reflection from a few crowns and crown boundaries, suggesting that the pixel size should be smaller than the smallest crown size for this method.

Systematic limitations may also be responsible for the lower estimation accuracy in coarser images. In the Spatial Analyst extension of ArcGIS 10, the intervals of the radius of opening cannot be less than the pixel size of the input data. As the pixel size increases, the number of classes that the estimated tree crown size can be assigned to declines, which increases the difficulty of discriminating finer differences. In our study, only three different opening sizes (1.60 m, 3.20 m, and 4.80 m in radius) were able to be assigned within the range of the maximum tree crown size for the 1.60-m pixel size image. The R^2 for the pixel size of 1.60 m was as low as 0.46,

suggesting that a pixel size larger than one third of the maximum crown radius may not be suitable for the method proposed in this study.

Implications for Conservation

Aichi Biodiversity Target 11 commits parties of the Convention on Biological Diversity to conserve more areas of particular importance for biodiversity, such as tropical forests, through effectively and equitably managed, ecologically representative, and well-connected systems of protected areas (Convention on Biological Diversity [CBD], 2010). The tree crown size over the large forest area can be used not only as the first screening of the candidates of mature or old growth forests but also as basic information for management planning. Because remote sensing can be a cost-efficient method to monitor the tree crown size and its spatial heterogeneity, developing such a method that is applicable over a wider range of forest conditions would meet the conservation purposes.

Potential for Utilizing Various Sensors and Low-Cost Monitoring

Several remote sensing methods have been developed for forest monitoring, such as multispectral or hyperspectral methods, which distinguish finer differences of vegetation by using more than two spectral bands (Ishii & Washitani, 2007; Martin, Newman, Aber, & Congalton, 1998; Pettorelli et al., 2005; Sader, Waide, Lawrence, & Joyce, 1989), as well as airborne laser scanning methods, which acquire a 3-D model of the canopy surface (Hyypä et al., 2008; Weishampel, Hightower, Chase, & Chase, 2012). Compared with these methods, which require specific types of data and are thus expensive, the method proposed in this study enables crown size estimations using monochrome data within a certain range of pixel sizes, such as the aerial images acquired by various institutions or high spatial resolution satellite images provided by IKONOS (1-m ground resolution in panchromatic mode) or Quickbird (0.6-m ground resolution in panchromatic mode; Ke & Quackenbush, 2011). Historical images acquired by governments, local authorities, or companies can be used to analyze the history of the forest.

CSI measurements estimated with the method proposed in this study may contribute to low-cost forest inventories and biodiversity monitoring. Processing monochromatic aerial or satellite images is much more cost effective than acquiring and processing laser scanning data (Hummel, Hudak, Uebler, Falkowski, & Megown, 2011; Ke & Quackenbush, 2011).

Because many government offices, research institutions, and companies already use the software employed in this study (ArcGIS 10), the application of our methodology may not incur additional costs. This low total cost increases

the likelihood that our methodology will be utilized by local authorities or developing countries to evaluate or monitor forest biodiversity for conservation purposes.

Precautions for Applications to Large Areas

This study estimated the average tree crown size in a forest patch with a closed canopy under the assumption that aerial images are composed of brighter treetops and darker crown boundaries. Therefore, the estimation accuracy should be lower in open woodlands where aerial images are composed of tree crowns and bare grounds or in shrublands where small crowns are arranged closely and do not have discernible boundaries in aerial images. In addition, in a mixture stand of canopy tree species with different life history traits, different allometric relationships among species might lower estimation accuracies.

The relationship between the estimated tree crown size and the biodiversity at a local scale may vary because of different canopy layer species, topographies, or historical human activities. The study site was an inland evergreen broad-leaved forest; however, coastal forests in the same region are characterized by different flora and fauna than mature inland forests (Miyawaki, 2013) because they are composed of pioneer tree species, such as charcoal-tree or Luchu pine, which have wider crowns (Shukla & Ramakrishnan, 1986). Canopy tree species and past human interventions should be considered when interpreting the crown-size index map at larger spatial scales because a coarser mosaic of different forest types may be included.

Authors' Note

The commercial aerial photograph (photograph number: CKU20085X-C8B-12) and the 10-m DEM were obtained from the Geospatial Information Authority of Japan (<http://mapapps.gsi.go.jp/maplibSearch.do#1> and <http://fgd.gsi.go.jp/download/menu.php>, respectively). Figure 1 and 2 were created using the GIS data obtained from the Geospatial Information Authority of Japan (<https://fgd.gsi.go.jp/download/menu.php>) and the Ministry of Land, Infrastructure and Transport of Japan (<http://nlftp.mlit.go.jp/ksj/gml/datalist/KsjTmplt-A13.html>).

Acknowledgments

The authors thank Ishikawa Takuya, Kimura Mariko, and members of Amami Mongoose Busters for providing helpful advice regarding the field surveys. The authors also thank Nishiyama Yutaka, Inoue Tohki, Inoue Natsumi, and Shinohara Naoto for providing support with the fieldwork. We also thank an anonymous reviewer for the thoughtful comments and advices.

Declaration of Conflicting Interests

The author(s) declared no potential conflicts of interest with respect to the research, authorship, and/or publication of this article.

Funding

The author(s) disclosed receipt of the following financial support for the research, authorship, and/or publication of this article: This study was partially supported by the Environmental Technology Development Fund, which is funded by the Ministry of the Environment, Japan (Subject NO. 4-1409), and JSPS KAKENHI Grant Number 26292181.

References

- Aiba, S. I., & Kohyama, T. (1997). Crown architecture and life-history traits of 14 tree species in a warm-temperate rain forest: Significance of spatial heterogeneity. *Journal of Ecology*, 85, 611–624.
- Bengtsson, J., Nilsson, S. G., Franc, A., & Menozzi, P. (2000). Biodiversity, disturbances, ecosystem function and management of European forests. *Forest Ecology and Management*, 132, 39–50.
- Biodiversity Center of Japan (2010) *Biodiversity of Japan: A harmonious coexistence between nature and humankind*. Tokyo, Japan: Heibonsya.
- Bossuyt, B., Heyn, M., & Hermy, M. (2002). Seed bank and vegetation composition of forest stands of varying age in central Belgium: Consequences for regeneration of ancient forest vegetation. *Plant Ecology*, 162, 33–48.
- Brokaw, N. V. L., & Lent, R. A. (1999). Vertical structure. In: M. L. Hunter (ed.) *Maintaining biodiversity in forest ecosystems* (pp. 373–399). Cambridge, UK: Cambridge University Press.
- Brown, A. H. F., & Oosterhuis, L. (1981). The role of buried seed in coppicewoods. *Biological Conservation*, 21, 19–38.
- Burrascano, S., Keeton, W. S., Sabatini, F. M., & Blasi, C. (2013). Commonality and variability in the structural attributes of moist temperate old-growth forests: A global review (The natural pruning of branches and their biological preconditioning). *Forest Ecology and Management*, 291, 458–479.
- Butin, H., & Kowalski, T. (1983). Die natürliche Astreinigung und ihre biologischen Voraussetzungen [The natural pruning of branches and their biological preconditioning]. *European Journal of Forest Pathology*, 13, 428–439.
- Convention on Biological Diversity (CBD). (2010). *TARGET 11—Technical rationale extended (provided in document COP/10/INF/12/Rev.1)*. Retrieved from <https://www.cbd.int/sp/targets/rationale/target-11/>.
- Cockle, K. L., Martin, K., & Robledo, G. (2012). Linking fungi, trees, and hole-using birds in a neotropical tree-cavity network: Pathways of cavity production and implications for conservation. *Forest Ecology and Management*, 264, 210–219.
- Culvenor, D. S. (2002). TIDA: An algorithm for the delineation of tree crowns in high spatial resolution remotely sensed imagery. *Computers & Geosciences*, 28, 33–44.
- Dietze, M. C., Wolosin, M. S., & Clark, J. S. (2008). Capturing diversity and interspecific variability in allometries: A hierarchical approach. *Forest Ecology and Management*, 256, 1939–1948.
- Heinzel, J. N., Weinacker, H., & Koch, B. (2011). Prior-knowledge-based single-tree extraction. *International Journal of Remote Sensing*, 32, 4999–5020.
- Hermy, M., Honnay, O., Firbank, L., Grashof-Bokdam, C., & Lawesson, J. E. (1999). An ecological comparison between ancient and other forest plant species of Europe, and the implications for forest conservation. *Biological Conservation*, 91, 9–22.
- Hirata, Y. (2008). Estimation of stand attributes in *Cryptomeria japonica* and *Chamaecyparis obtusa* stands using quickbird panchromatic data. *Journal of Forest Research*, 13, 147–154.
- Honnay, O., Degroote, B., & Hermy, M. (1998). Ancient-forest plant species in western Belgium: A species list and possible ecological mechanisms. *Belgian Journal of Botany*, 130, 139–154.
- Hummel, S., Hudak, A., Uebler, E., Falkowski, M., & Megown, K. (2011). A comparison of accuracy and cost of LIDAR versus stand exam data for landscape management on the Malheur national forest. *Journal of Forestry*, 109, 267–273.
- Hyypä, J., Hyypä, H., Leckie, D., Gougeon, F., Yu, X., & Maltamo, M. (2008). Review of methods of small-footprint airborne laser scanning for extracting forest inventory data in boreal forests. *International Journal of Remote Sensing*, 29, 1339–1366.
- Iida, Y., Kohyama, T. S., Kubo, T., Kassim, A. R., Poorter, L., Sterck, F., & Potts, M. D. (2011). Tree architecture and life-history strategies across 200 co-occurring tropical tree species. *Functional Ecology*, 25, 1260–1268.
- Ishii, J., & Washitani, I. (2007). Habitat analyses of six threatened plant species in a moist tall grassland based on hyperspectral-remotely sensed data. *Global Environmental Research-English Edition*, 11, 161–169.
- Jones, H. G., & Vaughan, R. A. (2010). *Remote sensing of vegetation: Principles, techniques, and applications*. Oxford, UK: Oxford University Press.
- Jonsell, M., Hansson, J., & Wedmo, L. (2007). Diversity of saproxylic beetle species in logging residues in Sweden—Comparisons between tree species and diameters. *Biological Conservation*, 138, 89–99.
- Kennedy, P. G., & Quinn, T. (2001). Understory plant establishment on old-growth stumps and the forest floor in Western Washington. *Forest Ecology and Management*, 154, 193–200.
- Ke, Y., & Quackenbush, L. J. (2011). A review of methods for automatic individual tree-crown detection and delineation from passive remote sensing. *International Journal of Remote Sensing*, 32, 4725–4747.
- Kira, T., & Shidei, T. (1967). Primary production and turnover of organic matter in different forest ecosystems of the western pacific. *Japanese Journal of Ecology*, 17, 70–87.
- Kruys, N., Fries, C., Jonsson, B. G., Lämås, T., & Ståhl, G. (1999). Wood-inhabiting cryptogams on dead Norway spruce (*Picea abies*) trees in managed Swedish boreal forests. *Canadian Journal of Forest Research*, 29, 178–186.
- Leckie, D. G., Gougeon, F. A., Walsworth, N., & Paradine, D. (2003). Stand delineation and composition estimation using semi-automated individual tree crown analysis. *Remote Sensing of Environment*, 85, 355–369.
- Martin, M. E., Newman, S. D., Aber, J. D., & Congalton, R. G. (1998). Determining forest species composition using high spectral resolution remote sensing data. *Remote Sensing of Environment*, 65, 249–254.
- Matsumoto, H., Ishii, J., Ohtani, M., & Washitani, I. (2014). Identification of forest areas of high conservation value using the crown size index: A case study in secondary beech forests at the northern range limit. *Japanese Journal of Conservation Ecology* (in Japanese), 19, 67–77.

- Miyawaki, A. (2013). *Vegetation of Japan, Okinawa and Ogasawara* (in Japanese). Tokyo, Japan: Shibundo.
- Nagendra, H., Lucas, R., Honrado, J. P., Jongman, R. H. G., Tarantino, C., Adamo, M., & Mairota, P. (2013). Remote sensing for conservation monitoring: Assessing protected areas, habitat extent, habitat condition, species diversity, and threats. *Ecological Indicators*, 33, 45–59.
- Naha Nature Conservation Office. (2008). *Basic points of views on conservation and utilization of natural resources in Amami region (draft)* (in Japanese). Retrieved February 8, 2016, from https://kyushu.env.go.jp/naha/nature/mat/data/m_3/m_3_3_3.pdf
- Nilsson, S. G., Niklasson, M., Hedin, J., Aronsson, G., Gutowski, J. M., Linder, P., . . . Raniush, T. (2002). Densities of large living and dead trees in old-growth temperate and boreal forests. *Forest Ecology and Management*, 161, 189–204.
- Ohsawa, M. (1990). An interpretation of latitudinal patterns of forest limits in South and East Asian mountains. *The Journal of Ecology*, 78, 326–339.
- Peterken, G. F. (1974). A method for assessing woodland flora for conservation using indicator species. *Biological Conservation*, 6, 239–245.
- Peterken, G. F. (1996). *Natural woodland: Ecology and conservation in northern temperate regions*. Cambridge, UK: Cambridge University Press.
- Pettorelli, N., Vik, J. O., Mysterud, A., Gaillard, J.-M., Tucker, C. J., & Stenseth, N. C. (2005). Using the satellite-derived NDVI to assess ecological responses to environmental change. *Trends in Ecology & Evolution*, 20, 503–510.
- Pickett, S. T. A., & White, P. S. (1985). *The Ecology of natural disturbance and patch dynamics*. New York, US: Academic Press.
- Pouliot, D., & King, D. (2005). Approaches for optimal automated individual tree crown detection in regenerating coniferous forests. *Canadian Journal of Remote Sensing*, 31, 255–267.
- R Development Core Team. (2013). *R: A language and environment for statistical computing*. Retrieved February 16, 2016, from <https://cran.r-project.org/bin/windows/base/old/3.0.1/>
- Rodrigues, A. S. L., Akçakaya, H. R., Andelman, S. J., Bakarr, M. I., Boitani, L., Brooks, T. M., . . . Yan, X. (2004). Global gap analysis: Priority regions for expanding the global protected-area network. *BioScience*, 54, 1092–1100.
- Sader, S. A., Waide, R. B., Lawrence, W. T., & Joyce, A. T. (1989). Tropical forest biomass and successional age class relationships to a vegetation index derived from landsat TM data. *Remote Sensing of Environment*, 28, 143–198.
- Shukla, R. P., & Ramakrishnan, P. S. (1986). Architecture and growth strategies of tropical trees in relation to successional status. *The Journal of Ecology*, 74, 33–46.
- Soille, P. (2004). *Morphological image analysis: Principles and applications*. Berlin, Germany: Springer Berlin Heidelberg.
- Song, C. (2007). Estimating tree crown size with spatial information of high resolution optical remotely sensed imagery. *International Journal of Remote Sensing*, 28, 3305–3322.
- Song, C., Dickinson, M. B., Su, L., Zhang, S., & Yaussey, D. (2010). Estimating average tree crown size using spatial information from Ikonos and QuickBird images: Across-sensor and across-site comparisons. *Remote Sensing of Environment*, 114, 1099–1107.
- Song, C., & Woodcock, C. E. (2003). Estimating tree crown size from multiresolution remotely sensed imagery. *Photogrammetric Engineering & Remote Sensing*, 69, 1263–1270.
- Speight, M. C. D. (1989). *Saproxylous invertebrates and their conservation*. Strasbourg, France: Council of Europe.
- Stokland, J. N., Siitonen, J., & Jonsson, B. G. (2012). *Biodiversity in dead wood*. Cambridge, UK: Cambridge University Press.
- Tagawa, H. (1995). Distribution of *Lucidophyll* Oak-Laurel forest formation in Asia and other areas. *Tropics*, 5, 1–40.
- Takahashi, M., Sakai, Y., Ootomo, R., & Shiozaki, M. (2000). Establishment of tree seedlings and water-soluble nutrients in coarse woody debris in an old-growth *Picea abies* forest in Hokkaido, Northern Japan. *Canadian Journal of Forest Research*, 30, 1148–1155.
- Turner, I. M., & Corlett, R. T. (1996). The conservation value of small, isolated fragments of lowland tropical rain forest. *Trends in Ecology & Evolution*, 11, 330–333.
- Wang, L., Gong, P., & Biging, G. S. (2004). Individual tree-crown delineation and treetop detection in high-spatial-resolution aerial imagery. *Photogrammetric Engineering & Remote Sensing*, 70, 351–357.
- Weishampel, J. F., Hightower, J. N., Chase, A. F., & Chase, D. Z. (2012). Use of airborne LiDAR to delineate canopy degradation and encroachment along the Guatemala-Belize border. *Tropical Conservation Science*, 5, 12–24.
- Whitman, A. A., & Hagan, J. M. (2007). An index to identify late-successional forest in temperate and boreal zones. *Forest Ecology and Management*, 246, 144–154.
- Whitney, G. G., & Foster, D. R. (1988). Overstorey composition and age as determinants of the understorey flora of woods of central New England. *The Journal of Ecology*, 76, 867–876.
- Winter, S., & Möller, G. C. (2008). Microhabitats in lowland beech forests as monitoring tool for nature conservation. *Forest Ecology and Management*, 255, 1251–1261.
- Wulder, M., Niemann, K. O., & Goodenough, D. G. (2000). Local maximum filtering for the extraction of tree locations and basal area from high spatial resolution imagery. *Remote Sensing of Environment*, 73, 103–114.